UNIVERSITY OF CALIFORNIA, SAN DIEGO

Paleomagnetic results from Costa Rica, Jan Mayen and Spitsbergen: An investigation of paleosecular variation over the last 10 Ma

A thesis submitted in partial satisfaction of the
requirements for the degree
Master of Science

in

Earth Sciences

by

Geoffrey John Deustua Cromwell

Committee in charge:

Professor Lisa Tauxe, Chair
Professor Steve Cande
Professor Paterno Castillo

2010

The thesis of Geoffrey John Deustua Cromwell is approved, and it is acceptable in quality and form for publication on microfilm and electronically:

_____

_____

_____

Chair

University of California, San Diego

2010

TABLE OF CONTENTS

LIST OF FIGURES

LIST OF TABLES

ACKNOWLEDGEMENTS

The thesis author would like to thank his advisor, Lisa Tauxe, for her support and commitment in helping him finish this project. The author is extremely grateful to her for the opportunity to study paleomagnetism and become a better scholar and scientist. The author would also like to thank his family and his friends at SIO for their support and encouragement during the last two years.

We thank Winfried Dallmann for his extensive field camp and logistical support on Spitsbergen. We thank Phil Gans for his personal communications regarding the ages of our Costa Rica samples. We thank Guillermo Alvarado-Induni and Wendy Perez for their logistical support in Costa Rica. We thank Leif-Erik Pedersen and Philip Staudigel for their hard work in the field collecting samples on Jan Mayen. We are grateful to the crew of Jan Mayen, especially Ole Øiseth and Filip Myrvoll, for their hospitality and expertise during our 2009 field season. We thank Jason Steindorf for his contributions in sample preparation and processing. We thank Stephen Peter for training and troubleshooting the ProMark3 GPS system. This research was supported by NSF grants EAR9805164 and EAR0838257

This thesis, in part is currently being prepared for submission for publication of the material. Cromwell, G., L. Tauxe, H. Staudigel, C.G. Constable, A. Koppers, R.-B. Pedersen. The thesis author was the primary investigator and author of this material.

VITA

2008	B. A. in Geology, Occidental College, Los Angeles, CA
2010	M. S. in Earth Sciences, Scripps Institution of Oceanography, University of California, San Diego

ABSTRACT OF THE THESIS

Paleomagnetic results from Costa Rica, Jan Mayen and Spitsbergen: An investigation of paleosecular variation over the last 10 Ma

by

Geoffrey John Deustua Cromwell

Master of Science in Earth Sciences

University of California, San Diego, 2010

Professor Lisa Tauxe, Chair

Paleosecular variation (PSV) models require high-quality, globally distributed paleomagnetic data sets in order to accurately predict observed geomagnetic field behavior. Previous paleomagnetic studies have lacked modern high-quality directional data, especially at equatorial and high northern latitudes. As a result of these incomplete data sets, PSV models, notably Model G [McFadden et al., 2008] and TK03 [Tauxe and Kent, 2004], may not accurately predict PSV behavior. We present 65 high-quality directional paleomagnetic sites from low (Costa Rica) and high northern (Jan Mayen and Spitsbergen) latitudes. We also compile a new paleomagnetic data set, PSV10, and investigate VGP dispersion with latitude. PSV10 spans the last 10 Ma and includes all published studies that meet our se-

lection criteria. We do not incorporate a latitudinal VGP cutoff and include all sites regardless of VGP latitude, so long as the published study does not intentionally sample transitional directions. Transitional directions are a natural aspect of secular variation, and removing them biases PSV behavior, especially at high latitudes where scatter is greater. Model G and TK03 underestimate dispersion of virtual geomagnetic poles (VGPs), of PSV10, at high and low latitudes. Attempts to modify the model parameters of Model G and TK03 to fit PSV10 were unsuccessful. PSV10 shows significant latitudinal variation between equatorial and high latitude sites, while dispersion across low to mid-latitudes is fairly consistent New PSV models must be developed to explain the observed behavior of the magnetic field.

Chapter 1

1.1 Introduction

Secular variation of the geomagnetic field has been observed since 8^{th} century, but only in the twentieth century has enough paleomagnetic data become available to develop detailed models of geomagnetic field behavior prior to the beginning of systematic human measurements in the 17^{th} century (e.g, Jackson et al. [2000]). Early studies of paleosecular variation (PSV) identified a latitudinal variation in directions and virtual geomagnetic poles (VGPs). The first PSV models, Model B [Creer et al., 1959] and Model A [Irving and Ward, 1964] assume that PSV derives from perturbations of an essentially dipolar field. While Model B perturbed the axis of the dipole field (dipole wobble), Model A perturbed dipole field vectors with a uniform distribution of non-dipole field directions.

The most cited PSV model is Model G [McFadden et al., 1988; McFadden et al., 1991; McElhinny et al., 1997] which uses the scatter parameter of Cox [1969], S, to quantify VGP dispersion. S is defined as:

$$S^2 = (N-1)^{-1} \sum_{i=1}^{N} (\Delta_i)^2, \tag{1.1}$$

where N is the number of observations and Δ is the angle between the i^{th} VGP and the spin axis. The Model G prediction for scatter is given by:

$$S = \sqrt{A^2\lambda^2 + B^2}, \tag{1.2}$$

where λ is latitude, and A and B are fitted parameters that reflect the contributions from the dipole and quadrupole families, respectively.

The next series of models, CP88, QC96, CJ98 and TK03 [Constable and Parker, 1988; Quidelleur and Courtillot, 1996; Johnson and Constable, 1995; Tauxe and Kent, 2004], rely on a "Giant Gaussian Process" (GGP) whereby gauss coefficients are drawn from normal distributions to predict both direction and intensity with standard deviation σ_l^m for each degree l and order m. In the most recent of these models, TK03 [Tauxe and Kent, 2004] there are three parameters: the average axial dipole term $\bar{g}_1^0$; α, defined by Constable and Parker [1988] as:

$$\sigma_l^2 = \frac{(c/a)^{2l}\alpha^2}{(l+1)(2l+1)}, \tag{1.3}$$

where c/a is the ratio of core radius to Earth radius; and β (defined as the ratio $\frac{\sigma_l^m(l-m:odd)}{\sigma_l^m(l-m:even)}$ for a given degree l). With the exception of CP88, the GGP style models were designed to predict VGP dispersion that is dependent on latitude.

The data sets used to parameterize Model G and subsequent PSV models all suffer from several drawbacks. Laboratory methods used for the majority of published paleomagnetic data are well below modern practice (e.g. McElhinny et al. [1997]). McElhinney et al. [1997] (hereafter MM97) suggested that ideal reliability criteria for selection of data include stepwise alternating field (AF) and thermal demagnetization and interpretation using principle component analysis [Kirschvink, 1980] . MM97 labeled data collected in such a manner as having a Demagnetization Code (DC) of 4 (see also McElhinny and McFadden [2000]). The PSVRL database [MM97] contained only 440 sites with DC codes ≥ 4 (out of 3719 total). In particular, there are no paleomagnetic data meeting minimum reliability standards available at latitudes $> 65°$, yet it is the high latitude scatter that is a critical aspect of the PSV models. Moreover, all data with VGPs within 45° of the equator are excluded from the PSVRL database of MM97. Since the compilation of the original PSVRL database by MM97, a concerted effort has been made to standardize laboratory methods and use principle component analysis during demagnetization. As a result, a recent data compilation [Johnson et al., 2008] contains 2107 individual sites with DC$\geq$ 4.

While the quantity of modern directional data has improved considerably, there is a lack of consensus in the paleomagnetic community as to what constitutes

high-quality site level data. The majority of selection criteria set forth by MM97 for their PSVRL database is virtually agreed upon by most paleomagnetists. For example, Johnson et al. [2008] used the following acceptance critera in their data compilation:

1. only data from lavas or thin dykes,
2. no regional tectonic effects,
3. $n \geq 5$ samples per site,
4. stability of magnetization,
5. 45° VGP cutoff,
6. DC ≥ 4, and
7. $\kappa \geq 50$.

The differences in selection criteria between Johnson et al. [2008] and those of MM97 are 1) n, the minimum number of samples per site, 2) the demagnetization code and 3) Johnson et al. [2008] used a cutoff of κ, while MM97 used a cutoff based on α_{95}.

In order to perform a meaningful evaluation of the geomagnetic field, we require a robust, high-quality data set that includes high latitude data. To this end, Johnson et al. [2008] made a compilation meeting the above critera. However, for certain regions, sites were included that had fewer samples per site. VGP dispersion as a function of latitude estimated from the compilation showed the surprising result that there was little variation of scatter with latitude in stark disagreement with predictions from most PSV models (with the notable exception of CP88). Johnson et al. [2008] concluded with the following statement: "Improved evaluation of existing models would be possible with larger low-latitude data sets and new data from high northern latitude". The data set compiled by Johnson et al. [2008] contains no high northern latitude data and only 34 high southern latitude sites.

Since the publication of Johnson et al. [2008], there have been new results published for lava flows from the last five million years (e.g. Lawrence et al. [2008], Opdyke et al. [2010], Sbarbori et al. [2009], Quidelleur et al. [2009], Tanaka et al. [2009], Calvo-Rathert et al. [2009])). Here, we present new high northern latitude paleomagnetic data from the islands of Jan Mayen and Spitsbergen, and a re-analysis of samples from Costa Rica (previously referenced as Constable et al. [in progress] in Johnson et al. [2008]). Our new directional data, along with the recently published datasets, greatly expand the available global and temporal resolution of PSV datasets.

In the present compilation we include all the directional data ignoring the VGP cutoff used routinely in previous compilations. The use of arbitrary VGP cutoffs may bias the interpretation of PSV and time average field properties [Clement, 2000; Coe et al., 2000; Lawrence et al., 2009], especially at high latitudes where the scatter is greater than at equatorial latitudes [Harrison, 2009; Lawrence et al., 2009]. We believe that excursions and reversals are inherent to secular variation and that transitional directions should not be excluded from PSV studies. We re-evaluate the nature of VGP dispersion and whether or not PSV models agree with our new high-quality data compilation. Note that studies that deliberately target excursional or transitional directions were not included in our compilation. Moreover, we have scoured the literature for studies meeting our selection criteria that were excluded in previous compilations (e.g. Udagawa et al. [1999], Yamamoto and Tsunukawa [2005], Ceja et al. [2006]). Finally, we have included sites with ages between five and 10 Ma, and adjusted these for plate motion in order to attain an accurate account of PSV.

1.2 Geology and Sampling

1.2.1 Costa Rica

Costa Rica is in southern Central America (Figure 1.1), between Nicaragua and Panama. Volcanism is attributed to the subduction of the Cocos plate beneath the Caribbean plate. The mid-late Miocene Cordellera de Talamaca is the

largest mountain belt in Costa Rica and consists of mid-Oligocene gabbros to Plio-Pleistocene volcanics [Drummond et al., 1995]. Our sampling efforts were focused in this volcanic belt. We sampled 39 young volcanic sites, predominantly ignimbrites and andesitic lavas, over two field seasons (1998, 2000). These were sampled with a gasoline powered drilled and oriented with both magnetic and sun compasses.

1.2.2 Jan Mayen

The island of Jan Mayen sits in the North Atlantic Ocean, just south of the Jan Mayen Fracture Zone between the Mohns and Kolbeinsey Ridges (Figure 1.2). Jan Mayen is a volcanic island dominated by the Earth's northermost active volcano, Beerenberg. Surface volcanism is believed to be Bruhnes age or younger [Imsland, 1978] based on a set of $^{40}K/^{40}Ar$ dates [Duncan, R., unpublished, Fitch et al., 1965]. Fitch et al., 1963 collected samples from ten cooling units on the flanks of Beerenberg. These behaved well during both thermal and alternating field demagnetization and are of uniformly normal polarity. The geology, geochemistry and petrology of the island is described extensively by Imsland [1978] and Imsland [1980] . Recently, the geochemistry of the island has been the subject of investigation on mantle composition and the behavior of the Iceland Mantle Plume [Schilling et al., 1999; Mertz et al., 2004; Debaille et al., 2009].

In August 2009 we took oriented samples from 23 ankaramitic basalt to basaltic lava flows and one basaltic dike (see Figure 1.2). Site selection was based on accesability by foot. Our sampling was guided by the sampling sites of the unpublished $^{40}K/^{40}Ar$ dates [Duncan, R., unpublished]. Care was taken not to collect samples where there was evidence of tilting, slumping or any frost heaving effects. Nearby/overlying lava flows were sampled only if a time gap could be determined in the field so as not to ovesample the same geomagnetic field. A minimum of 10, 2.5 cm diameter samples were collected at each site using a gasoline powered drill. Cores were oriented using magnetic compass, sun compass (when possible), and a ProMark3 differential GPS system (Figure 1.3). The ProMark3 GPS system allows for on-site, drill core azimuth calculation using a modified

Pomeroy with an attached laser. The Pomeroy is inserted around the drill core and the"Rover" GPS receiver takes three measurements along the path of the laser. The calculated azimuths are, on average, within 5° of the sun compass measurements. Benefits of this system over other differential GPS systems [Lawrence et al., 2009] include faster (2 min) per sample orientation time and less bulky equipment to carry.

1.2.3 Spitsbergen

Spitsbergen is an island in the northwest of the Svalbard archipelago, on the norwestern edge of the Barents shelf in the North Atlantic (Figure 1.2). The archipelago is defined by fold-thrust belts associated with Paleozoic tectonics [Lyberis et al., 1999; dwewy et al., 2003; Torsvik et al., 2001] and the cenozoic opening of the Norwegian-Greenland Sea [Talwani and Eldholm, 1977]. The geology of the island is discussed in Harland [1997] among others. Previous paleomagnetic work on Spitsbergen has been used to define apparent polar wander paths (APWs) from the Paleozoic [Jelenska, 1987; Maloof et al., 2006] through the Cenozoic [Nawrocki, 1999].There has not been a focus, until now, on recent volcanism.

We collected 13 sites in summer 2001 with ages ranging from very young to approximately 9 Ma [see Table 1.3]. Various lithologies were sampled including pahoehoe lava flows, xenoliths, palagonite tuffs and basalt dikes. At each site a minimum of 10, 2.5 cm diameter samples were drilled using a gasoline powered drill. Samples were oriented with a magnetic compass, sun compass (when possible) and differential GPS. The GPS system used was that described by Lawrence et al. [2009].

1.3 Methods & Results

1.3.1 Dating

Costa Rica

Samples from 13 sites were chosen for age determinations by $^{40}AR/^{39}Ar$ incremental heating experiments in the UC Santa Barbara Argon Laboratory [Gans, 2010] (see Table 1.1). Samples were crushed and sieved to 0.25 to 0.5 mm fraction and were then exposed to heavy duty ultrasonic treatment. Magnetic density separation and hand picking was performed to obtain pure groundmass. Unirradiated splits of most whole rock samples were first analyzed on the mass spectrometer to get a preliminary assessment of the age and expected radiogenic yields, and thus better plan the analytical strategy. More silicic units were first coarsly crushed and carefully hand-picked to remove as much of the xenolithic contamination as possible.

Depending on the age and potassium content, 20-400 mg of each sample were packaged for irradiation at the Oregon State research reactor [Gans, 2010]. The samples were divided into a younger group (estimated <500 ka) that was given a 10 minute irradiation. An older group was irradiated for 40 minutes. All the samples were monitored using Taylor Creek Rhyolite sanadine (assigned age 27.92 Ma).

Results were generally excellent, with ages of samples ranging from 13.5 ka to 2.0 Ma [Gans, 2010]. Groundmass concentrates from mafic lavas tended to yield typical "recoil" type spectra, with old apparent ages in low temperature steps, but generally well defined plateaus for the gas released at 800-1000 C. Plagioclase from more silicic units generally gave fairly flat release spectra with well defined plateaus, except in cases with obvious xenocrystic contamination [Gans, 2010].

Jan Mayen

Ages from $^{40}AR/^{39}Ar$ incremental heating experiments will be included in a later publication.

Spitsbergen

$^{40}AR/^{39}Ar$ incremental heating experiments were successful on samples from three sites (see Table 1.3). Dating was conducted at Oregon State University. Successful ages ranged from 8.3 to 9.17 Ma. Sites sp100-104, and sp106-108 are too young to date using this method. Sites sp110, sp112, and sp113 are part of the same lava flow sequence as sp109 and sp111 and are therefore assigned equivalent ages of 9 Ma.

1.3.2 Paleomagnetism

We measured directions of the natural remanent magnetization (NRM) for all specimens using either a 2G or CTF cryogenic magnetometer housed in the magnetically shielded room at Scripps Institution of Oceanography (SIO). At least five specimens per site were magnetically cleaned by stepwise alternating field (AF) and thermal demagnetization, using either the Sapphire Instruments SI-4 uniaxial AF demagnetizer or SIO home-buit ovens. Principal component analysis [Kirschvink, 1980] was used to determine characteristic directions or best fit planes for each specimen.

For AF experiments, in general, specimens were measured after demagnetization at the following steps: 5, 10,15, 20, 30, 40, 50, 60, 80, 100, 120, 150, 180 mT. Some specimens decayed quite rapidly and demagnetization was halted prior to 180 mT. Above peak fields of 80 mT, the Jan Mayen specimens (and 6 out of 32 specimens from Spitsbergen) were subjected to a "triple demagnetization" protocol [Stephenson, 1993; Tauxe, 2010] in order to counteract the effect of gyroremanent magnetization (GRM), a problem in anisotropic specimens. Costa Rica and the rest of the Spitsbergen specimens were not demagnetized with the GRM protocol. These were examined for evidence of GRM (acquisition of a component of magnetization orthogonal to the last axis demagnetized) and none was found.

In general, thermal demagnetization was carried out in steps of) 100, 150, 200, 250, 300, 350, 400, 450, 475, 500°C, followed by 10 steps from 510-610°C or until the maximum unblocking temperature was reached ($< 5\%$ of the NRM remaining). Many thermal demagnetization experiments were carried out in con-

junction with an IZZI modified Thellier-Thellier experiment [Tauxe and Staudidel, 2004; Yu et al., 2004] to obtain paleointensity information (to be published elsewhere).

Three types of site level demagnetization behavior were observed (Figure 1.4). Type I sites (16 total) decayed linearly to the origin in both AF and thermal demagnetization experiments (Figure 1.4a-c). Type II sites (30 total) were categorized by some thermal demagnetized specimens exhibiting significant deflection away from the origin during the IZZI experiments (Figure 1.4d-f). In this method specimens are heated repeatedly and alteration or unremoved pTRM tails deflect the remanence toward the laboratory field. These specimens (Figure 1.4(e)) display a "hedgehog" shape as they move first toward the lab field direction then toward the origin. We interpret data from Type II specimens with best fit planes under the assumption that the characteristic direction is contained within the plane. Type III sites (20 total) contain one or more specimens that display multi-component behavior in either AF or thermal demagnetization experiments (Figure 1.4g-i). Specimens from such sites are interpreted using either best-fit lines (Figure 1.4g) or best fit planes (Figure 1.4h).

Five deviant specimens (cr409b1, cr412c1, cr414la1, cr422j2, cr431a2) were determined to be misoriented during sampling [Tauxe, 2010] and were excluded from site mean analysis.

Site means were calculated based on best-field lines or planes with at least four consecutive demagnetization steps and a maximum angle of deviation (MAD) $\leq 5^{\circ}$. Average directions and concentration statistics (k) for those sites with only best fit lines were calculated using the method of Fisher [1953]. Best fit lines and planes were combined using the method of McFadden and McElhinny [1988]. Site level selection criteria is based on Johnson et al. [2008] (without the VGP cutoff) whereby $n \geq 5$ with at least one directed line, and $k \geq 50$, (see Tables 1.1, 1.2, and 1.3). Sites cr035, cr414l, cr414m, cr416, cr421, cr428, cr431 did not meet these criteria and were excluded from our analysis of VGP dispersion. Sites jm005, jm010, jm018 and cr413 were unoriented and are not suitable for paleodirections. In total, 66 sites from the three locations met our selection criteria. The site mean

directions and VGPs for our three study locations are shown in Figure 1.5.

We estimate the angular standard deviation of the scatter S of the VGPs from Costa Rica, Jan Mayen and Spitsbergen. In Table 1.4 we list S with no cutoff, the variable colatitude cutoff of Vandamme [1994] and a 45° cutoff. Costa Rica VGP scatter is consistent with other mid to low latitude studies, although not nearly as low as equatorial sites. Our calculation of scatter in Costa Rica remains essentially unchanged from prior publication of the data in Johnson et al. [2008] ($17.3^{22.0}_{12.6}$ [This Study], $17.5^{22.5}_{12.5}$ Johnson et al. [2008]) despite the inclusion of two new high-quality sites. We reanalyzed the paleomagnetic data from Costa Rica and determined that site cr414 was in fact three separate lava flows (cr414l, cr414m, cr414u) and that the orientation data for site cr035 was incorrectly labeled. Sites cr035 and cr414u are included in our site mean analysis, while cr414l and cr414m did not meet our acceptance criteria. All other sites are essentially unchanged. VGP dispersion at Jan Mayen and Spitsbergen correspond well with scatter in Antarctica [Lawrence et al., 2009], providing a northern hemisphere analogue to previous high southern latitude data.

1.4 Discussion

We present here an expanded, high quality, data compilation (PSV10) in order to evaluate the behavior of the geomagnetic field over the last 10 Ma. Previously constructed data sets (e.g., Mcelhinny et al. [1997], Johnson et al. [2008]) chose selection criteria that maximized the number of data points, and as a result included studies that were based on less stringent laboratory methods. The number of studies meeting the stricter selection criteria has increased such that it is now worthwhile considering only the highest quality data sets. Therefore, in this study, we required all sites to meet the same site level criteria, i.e., $n \geq 5$, $k \geq 50$. Each site must be based on specimens with Demagnetization Code ≥ 4, be free from any tilting or regional tectonic effects, and must not preferentially sample transitional directions. We selected studies younger than 10 Ma. Most other PSV compilations [Johnson and Constable, 1995; McElhinny et al., 1996; Lawrence et

al., 2009] select data younger than 5 Ma in order to neglect any plate motion and because of the decrease of data with age. Johnson et al. [2008] adjusted all the sites in that compilation for the NUVEL1 plate motion model [DeMets et al., 1994] . Several sites from Spitsbergen and Antarctica [Lawrenc et al., 2009] are late Miocene; hence we chose to include all sites (ours and in the published literature) younger than 10 Ma that fit our other criteria. Sites found between 5-10 Ma were corrected for plate motion using the predicted site latitudes of Besse and Courtillot, [2002] .

Many studies reject VGPs if they are more than 45° from the spin axis, or below the variable colatitude cutoff of Vandamme [1994] , in order to avoid overrepresentation of transitional directions. The use of arbitrary VGP cutoffs may, however, bias the interpretation of PSV and time average field properties [Clement, 2000; Coe et al., 2000; Lawrence et al., 2009] , especially at high latitude where the scatter is greater than at equatorial latitudes [Harrison, 2009; Lawrence et al., 2009] . We consider excursions and reversals to be inherent in secular variation and that deviant directions meeting our minimum criteria should not be excluded *a priori* from PSV studies. The exception to this rule is if transitional directions are specifically targeted during sampling. In all other cases we have excluded no directions and have added them back in to the database.

The PSV10 database consists of 1,836 independent sites from 72 different studies, including this study (see Figure **??**, Table 1.5, Table 1.6). Although recent efforts have been made to sample underrepresented regions of the globe (e.g. Opdyke et al. [2010], Lawrence et al. [2009] , This Study), there are still regions that lack sufficient high quality data, most notably at high latitudes in both hemispheres. There are significantly more sites in the northern hemisphere. No doubt that site accessibility in terms of geographic location and age (young, normal polarity, Bruhnes age lavas) contributes greatly to the global and temporal resolution of available high quality data. It is reasonable to assume that a good picture of VGP dispersion can be drawn from low to mid-latitude northern hemisphere data, however any discussion about the relationship between northern and southern latitudes must be placed on hold until more data is collected in the south.

We have taken the antipodes of the reverse VGPs and grouped the data in 10° latitudinal bins in Figure **??**. This practice obscures several important aspects of the data: polarity distribution and number of data in each bin. To overcome these drawbacks, we plot the individual VGP latitudes versus site latitudes in Figure 1.7. This type of presentation allows the reader to observe the latitudinal distribution of data, qualitative VGP dispersion and polarity.

The problem of temporal sampling (most of the studies in PSV10 span less than 1 Ma) biases the available records. It is possible that the observed lack of transitional directions in certain geographic locations is due to a limited temporal distribution. We see in Figure 1.7 that regions with a high volume of data, 20°S, 20°N and 40°N, show more transitional VGPs. Moreover, it might be possible that regions with a wider range of ages show more intermediate VGP latitudes. For example, the Antarctic data has a large number of data points and large age range; it also has a high dispersion of VGP latitudes. However a plot of age vs. site latitude (Figure 1.8) shows this is not the case. The equatorial data spans nearly as large an age range as Antarctica and has even more data points, yet there are fewer transitional VGPs.

In order to investigate latitudinal variation of VGP dispersion, we compare several existing statistical models (CP88, Model G, TK03) with the PSV10 data set. These models are all symmetric about the equator and are blind as to polarity, so we have taken the absolute values of both the VGP latitudes and the site latitudes and binned them in 10° latitudinal bins in Figure 1.9. It is evident in that the equatorial and high latitude sites are significantly lower and higher, respectively, than mid-latitude sites (Figures 1.6, 1.7, 1.9). The mid-latitude sites are not significantly different and it can be argued that they are not latitudinally dependent. CP88 (pink) predicts almost no latitudinal dependency and does not fit the PSV10 data set at all. TK03 (green) and Model G (red) woefully underestimate dispersion at high latitude because both models were designed to fit other data sets that did not include high latitude sites.

We adjust the parameters in TK03 and Model G in order to evaluate whether these simple statistical models might be fit to the new PSV10 data set. For

TK03' (blue), the parameters α/β were changed from 2.4/3.8 to 3.5/8.22. TK03' follows low latitude dispersion from 0 to 20 almost exactly, yet over estimates the mid-latitude regime. For Model G' (teal), the parameters a/b were changed from 0.23/12.9 to 0.35/12.9. Model G' performs slightly better as it follows the trend of the mid-latitude data but in doing so it underestimates lower latitude dispersion. The biggest issue with these simple statistical models is their parameters affect high and low ends of dispersion while lacking the ability to be finely tuned to unique latitudinal behavior. An ideal model might increase slightly from the equatorial dispersion value to about 17-18 and remain at that level until increasing sharply to accommodate the high latitude dispersion. None of the available models, in their current form, have the ability to fit PSV10. Future statistical models must allow enhanced latitudinal control over VGP scatter.

1.5 Conclusions

The directional analysis of new volcanic sites from Costa Rica, Jan Mayen and Spitsbergen provide 65 new high-quality sites with well constrained data ($n \geq 5$ and $k \geq 50$). Ages range from 0-2 Ma in Costa Rica, 0-400 ka in Jan Mayen, and 0-9 Ma in Spitsbergen. Uncut VGP dispersion in Costa Rica ($17.5^{22.2}_{13.1}$), Jan Mayen ($29.3^{35.6}_{22.9}$) and Spitsbergen ($28.1^{35.4}_{20.2}$) is consistent with studies at similar latitudes.

The PSV10 data set is a compilation of high-quality ($n \geq 5$, $k \geq 50$, DC≥ 4) directional studies from 0-10 Ma. All studies in PSV10 are free of tectonic activity and do not preferentially sample transitional directions. We choose to evaluate VGP dispersion of PSV10 with no cutoff angle. The use of a 45° or the variable Vandamme [1994] cutoff removes transitional directions that are a natural result of secular variation. Removing transitional directions biases the interpretation of paleosecular variation, especially at high latitude.

Statistical models TK03 and Model G underestimate dispersion of PSV10 at both low and high latitudes, while CP88 shows no latitudinal variation whatsoever. Attempts to fit TK03 and Model G by modifying the parameters α/β and a/b, respectively, were also unsuccessful because they fail to accurately pre-

dict VGP dispersion at all latitudes. VGP dispersion of the magnetic field is too complicated for these simple statistical models. There is significant latitudinal variation between equatorial and high latitude sites, while dispersion across low to mid-latitudes is fairly consistent. New statistical models must be developed to explain the observed behavior of the magnetic field.

Although the global distribution of high-quality paleomagnetic data has improved, the southern hemisphere and high latitude regions are sparsely sampled compared to northern, low and mid-latitudes. More data is necessary to obtain a more complete and reliable view of the magnetic field.

This thesis, in part is currently being prepared for submission for publication of the material. Cromwell, G., L. Tauxe, H. Staudigel, C.G. Constable, A. Koppers, R.-B. Pedersen. The thesis author was the primary investigator and author of this material.

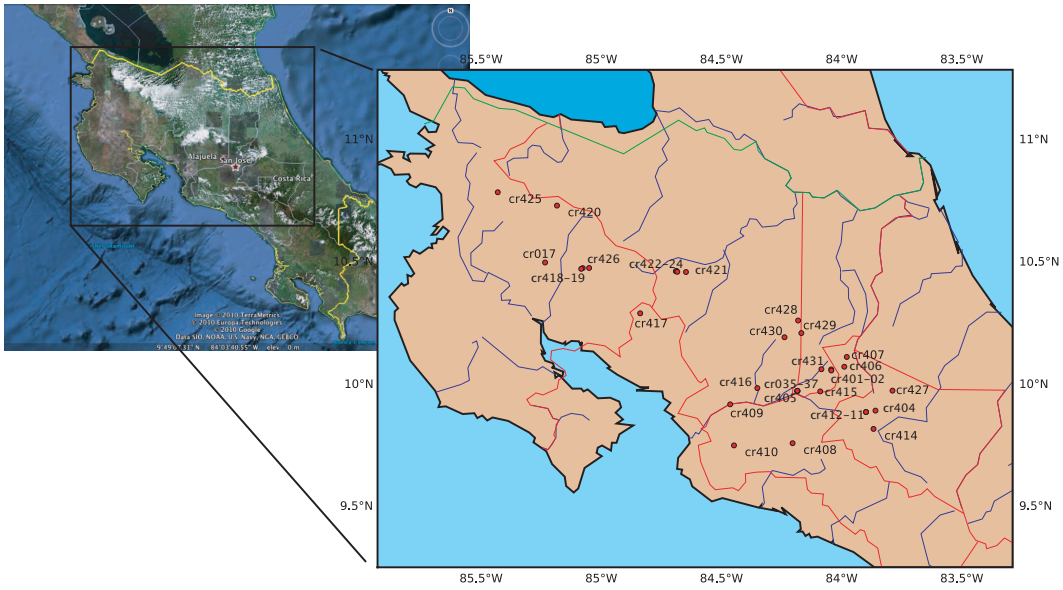

Figure 1.1: Google Earth image of Central America (Nicaragua, Costa Rica, Panama). Inset: Location map of sites from Costa Rica used in this study.

Table 1.1: Costa Rica site statistics. Ages from Gans [2010]. Age is the average $^{40}Ar/^{39}Ar$ radiometric age with 2σ error. Dec and Inc are mean site declination and inclination, respectively. nl/np is the number of best-fit lines and planes, respectively. N is the combined number of best-fit lines and planes of all the specimens used in site calculations. k is an estimate of the Fisher [1953] precision parameter, R is the resultant vector of N unit vectors, and $\alpha 95$ is the Fisher [1953] circle of 95% confidence. VGP Lat and Lon are the virtual geomagnetic poles calculated for each site.

Site	Age (ka)	Lat (°N)	Lon (°E)	Dec	Inc	nl/np/N	k	R	α^{95}	VGP Lat	VGP Lon
cr017	2110±20	10.50	-85.23	15.2	17.8	5/0/5	1196.4	4.9967	2.2	75.0	8.7
cr035		9.97	-84.18	358.5	21.5	4/7/11	327.2	10.9801	2.6	88.0	228.6
cr036	321±18	9.97	-84.18	353.2	23.4	5/1/6	149.0	5.9698	5.6	83.0	205.0
cr037	496±16	9.97	-84.18	357.7	28.4	9/2/11	106.8	10.9157	4.5	84.4	252.5
cr401	426±14	10.06	-84.04	347.1	-6.9	7/2/9	785.5	8.9911	1.9	71.3	140.1
cr402	427±6	10.06	-84.04	0.6	-22.7	6/0/6	142.4	5.9649	5.6	68.1	94.4
cr404	13.5±5	9.89	-83.86	347.2	5.4	6/2/8	340.4	7.9824	3.1	75.4	157.5
cr405	332±12	9.97	-84.18	355.4	21.7	7/3/10	433.1	9.9827	2.4	85.3	202.1
cr406		10.07	-83.98	0.8	22.5	6/3/9	1630.0	8.9960	1.3	88.2	301.7
cr407		10.11	-83.97	218.7	24.4	10/0/10	387.1	9.9768	2.5	-45.3	216.0
cr408	270±6	9.76	-84.2	14.2	4.9	1/6/7	160.0	6.9813	5.5	74.1	32.3
cr409	330.7±2	9.92	-84.46	340	21.6	7/2/9	128.1	8.9454	4.6	70.3	192.0
cr410		9.75	-84.44	349.1	23.5	6/4/10	58.2	9.8798	6.5	79.0	199.8
cr411		9.88	-83.89	22.5	-15.7	6/2/8	667.0	7.9910	2.2	61.3	43.9
cr412	176±2	9.88	-83.89	30.5	-4.4	7/1/8	322.4	7.9798	3.1	57.3	26.1
cr414l		9.82	-83.86	359.0	-14.9	4/0/4	1930.5	3.9984	2.1		
cr414m		9.82	-83.86	65.8	15.3	2/3/5	19.4	4.871	20.2		
cr414u		9.82	-83.86	13.2	-13.3	5/0/5	3405.3	4.9988	1.3	68.9	57.2
cr415	338±4	9.97	-84.08	359.0	9.3	8/0/8	223.8	7.9687	3.7	84.6	106.6
cr416		9.98	-84.35	163.6	-10.6	3/1/4	26.7	3.9064	19.2		
cr417		10.29	-84.83	22.2	35.4	5/1/6	124.2	5.9638	6.1	66.7	339.2
cr418		10.47	-85.07	180.6	-8.2	11/0/11	992.7	10.9899	1.4	-83.6	269.5
cr419		10.47	-85.07	352.5	33.5	5/0/5	207.6	4.9807	5.3	79.3	233.0
cr420		10.73	-85.18	7.6	31.4	11/0/11	951.9	10.9895	1.5	80.3	323.7
cr421		10.46	-84.64	347.7	43.4	2/4/6	15.2	5.8024	19.7		
cr422-423		10.46	-84.68	348.7	32.8	14/2/16	846	15.9823	1.4	76.8	220.6
cr424		10.46	-84.68	7.0	11.8	4/3/7	792.7	6.9943	2.2	81.7	37.8
cr425		10.78	-85.42	184.6	-17.4	4/1/5	349.8	4.9900	4.2	-85.1	206.7
cr426	2032±10	10.47	-85.05	173.6	8.3	7/1/8	272.7	7.9762	3.4	-74.0	298.8
cr427		9.97	-83.78	359.8	43.8	7/2/9	560.3	8.9875	2.2	74.4	275.5
cr428		10.26	-84.18	291.7	6.3	6/1/7	38.4	6.8567	10.0		
cr429	61±2	10.21	-84.16	357.0	31.8	6/0/6	259.8	5.9808	4.2	82.4	253.6
cr430		10.19	-84.23	356.9	26.2	6/3/9	528.1	8.9877	2.3	85.3	236.2
cr431		10.06	-84.08	7.5	7.1	2/3/5	29.5	4.9153	16.2		

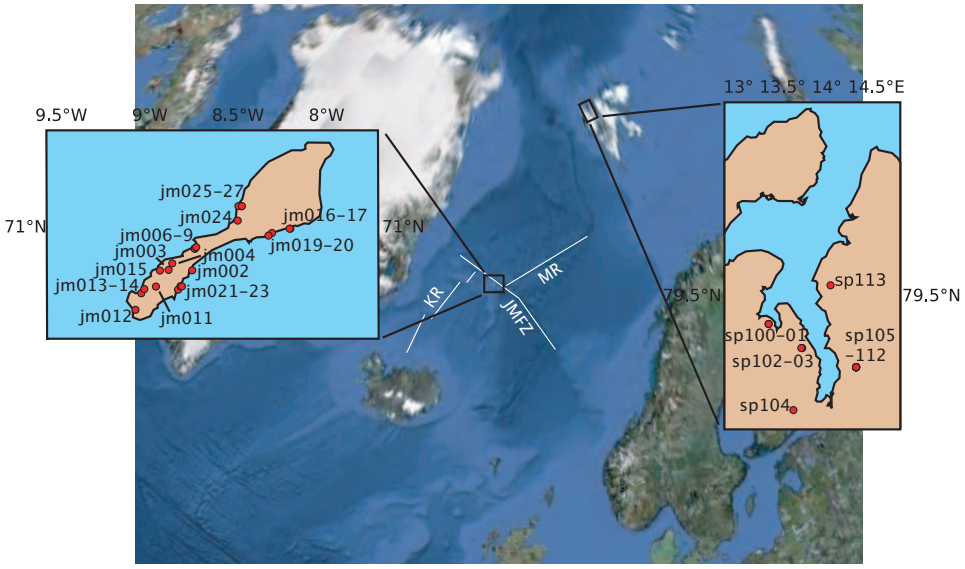

Figure 1.2: Google Earth image of the North Atlantic region. Left inset: Location map of sites from Jan Mayen. Right inset: Location map of sites from Spitsbergen. KR is Kolbeinsey Ridge, MR is Mohns Ridge, JMFZ is Jan Mayen fracture Zone.

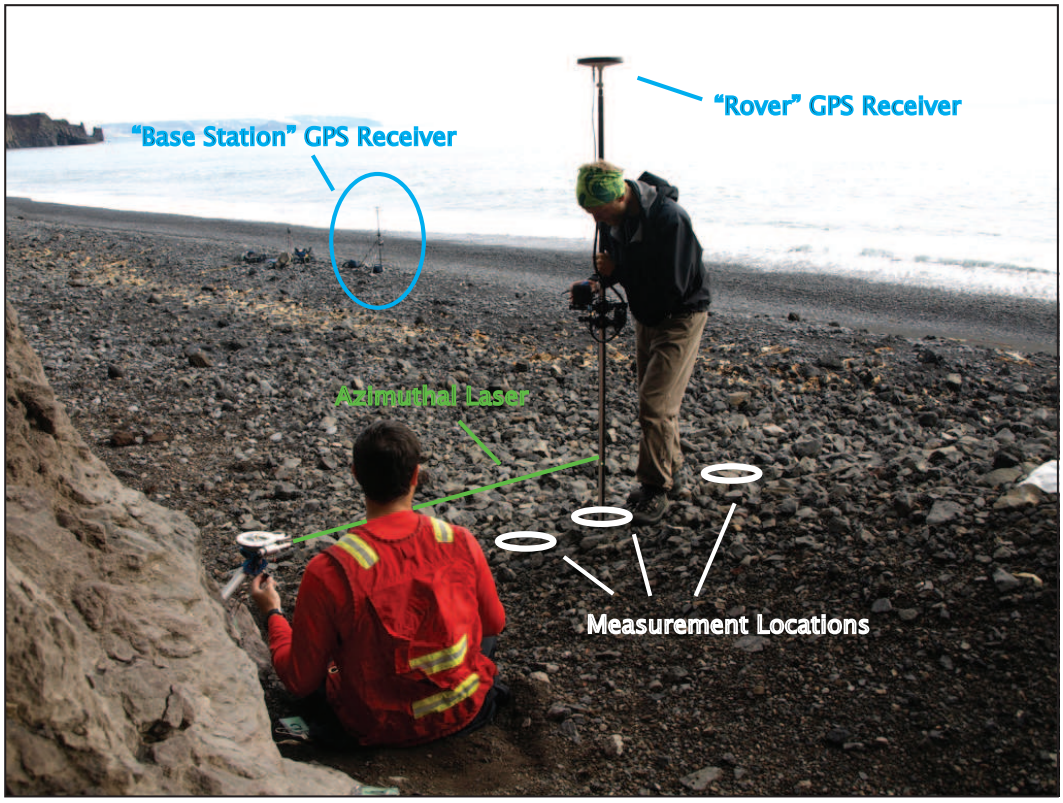

Figure 1.3: Image of differential GPS system for orienting paleomagnetic samples in regions with significant cloud cover. The "Rover" takes location measurements at three points along the azimuthal laser. The azimuth of the paleomagnetic drill core is determined in the field or during post-processing.

Table 1.2: Jan Mayen site statistics. See Table 1.1 for a description of statistics

Site	Age (ka)	Lat (°N)	Lon (°E)	Dec	Inc	nl/np/N	k	R	$\alpha 95$	VGP Lat	VGP Lon
jm002		70.91	-8.72	61.8	75.5	5/4/9	236.8	8.9747	3.5	65.6	69.4
jm003		70.92	-8.85	354.5	80.7	5/2/7	250.2	6.9800	3.9	88.0	292.0
jm004		70.93	-8.83	3.9	76.9	5/2/7	304.5	6.9836	3.6	83.9	155.4
jm006		70.96	-8.70	302.3	72.6	5/1/6	409.1	5.9890	3.4	63.3	262.3
jm007		70.96	-8.70	66.3	83.6	5/2/7	673.1	6.9926	2.4	72.0	31.7
jm008		70.96	-8.70	1.5	85.7	4/2/6	191.8	5.9791	5.1	79.5	352.5
jm009		70.96	-8.69	51.5	83.0	8/0/8	147.6	7.9526	4.6	75.1	37.9
jm011		70.89	-8.92	86.6	80.9	6/4/10	82.3	9.9150	5.5	64.9	37.0
jm012		70.85	-9.04	56.4	64.7	6/187	550.2	6.9900	2.6	54.2	92.9
jm013		70.88	-9.00	22.9	78.9	8/0/8	154.5	7.9547	4.5	81.8	86.2
jm014		70.92	-8.99	47.0	63.6	5/1/6	54.1	5.9168	9.4	55.9	104.3
jm015		71.00	-8.90	294.5	79.5	6/0/6	86.4	5.9421	7.2	68.9	289.4
jm016		71.00	-8.16	179.0	66.9	5/1/6	307.5	5.9854	3.9	30.5	352.6
jm017		70.99	-8.16	353.4	77.4	7/0/7	240.6	6.9751	3.9	84.4	200.4
jm019		70.99	-8.26	93.5	63.3	6/4/10	482.1	9.9855	2.3	40.7	60.8
jm020		70.98	-8.28	61.2	79.9	5/1/6	146.2	5.9692	5.7	70.6	54.1
jm021		70.88	-8.80	95.6	72.3	8/0/8	622.0	7.9887	2.2	51.2	49.9
jm022		70.89	-8.78	97.5	62.9	3/3/6	823.0	5.9957	2.5	39.0	57.1
jm023		70.89	-8.77	329.1	67.7	5/0/5	67.2	4.9404	9.4	65.3	222.5
jm024		71.01	-8.46	302.7	79.5	4/3/7	73.6	6.9389	7.4	71.4	285.1
jm025		71.04	-8.44	80.2	75.0	5/2/7	1234.2	6.9959	1.8	59.3	57.2
jm026		71.04	-8.45	36.0	73.8	6/1/7	914.6	6.9940	2.0	71.8	100.8
jm027		71.04	-8.43	242.1	81.4	5/1/6	797.1	5.9944	2.4	59.5	321.3

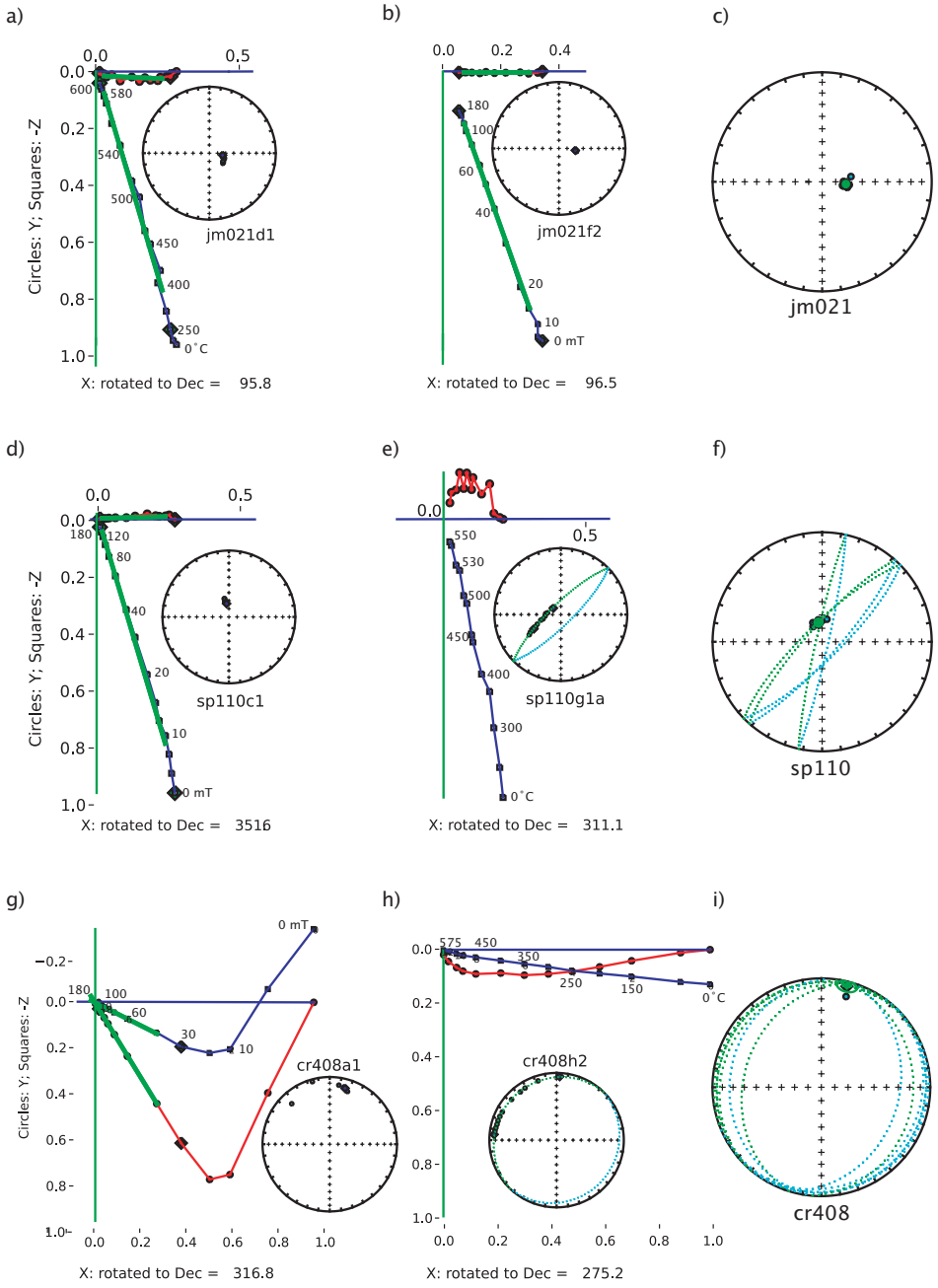

Figure 1.4: (a-c) Typical "Type I" site. a) Thermal demagnetization shows straightforward, univectorial decay to the origin. Inset is plot of directions from each demagnetization step. b) AF demagnetization of sister specimen. Behavior is similar to thermal demagnetization. Inset same as a). c) Directions of all best-fit lines defining characteristic directions similar to a) and b), site mean (green circle). (d-f) "Type II" site. d) AF or thermal (not shown) demagnetization shows univectorial decay to the origin. Inset same as in a). e) Demagnetization derived from Thellier (IZZI) experiment showing contamination from the applied lab field. Inset shows directions at each demag step plotting as a great circle rather than a best-fit line. f) Same as c) except including great circle fits. (g-i) "Type III" site. g) AF demagnetization showing a characteristic remanent magnetization decaying to the origin. Inset same as a). h) Thermal or AF (not shown) demagnetization displaying multi-component behavior. Inset same as in e). i) Same as in f).

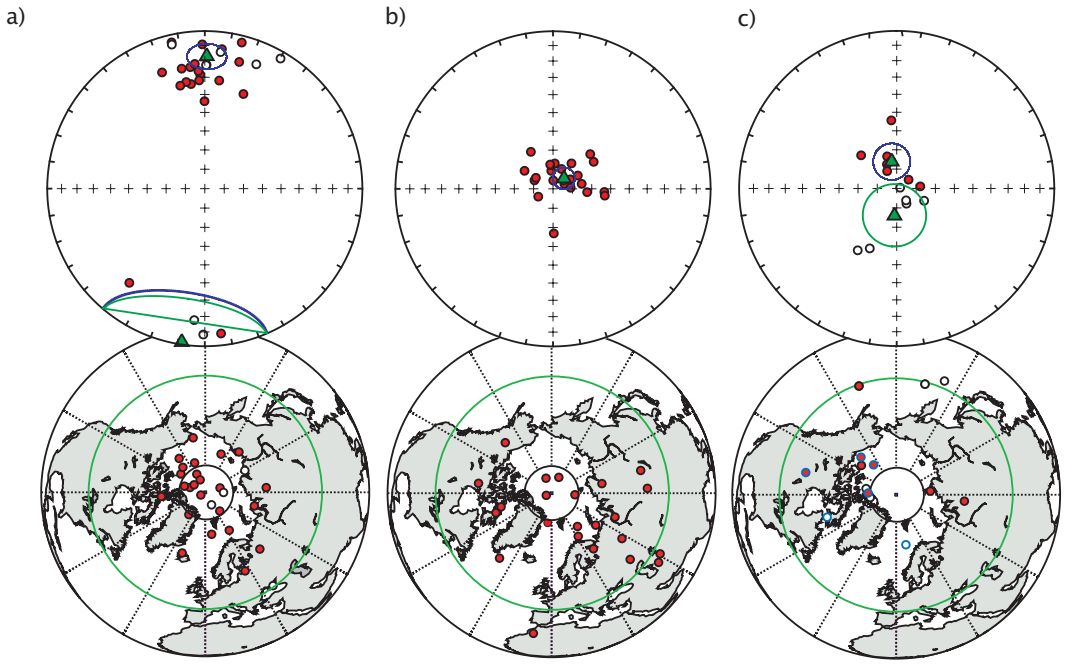

Figure 1.5: a) Costa Rica. b) Jan Mayen. c) Spitsbergen. Top: Equal area projections of site-mean directions. Filled (open) circles plot on the lower (upper) hemisphere. Mean directions (green triangles) with Fisher a95 confidence cones for normal (blue circle) and reversed (green circle) sites. Bottom: VGP positions for all sites meeting site selection criteria. Filled (open) circles are positive (reversed, anti-podal) VGP positions. VGPs are presented with no latitude cutoff. VGPs outlined in blue are older than 5 Ma and have been corrected for plate motion. Green circle is 45° latitude from the pole. VGPs lying below this circle would have been rejected in studies using a 45° latitude cutoff.

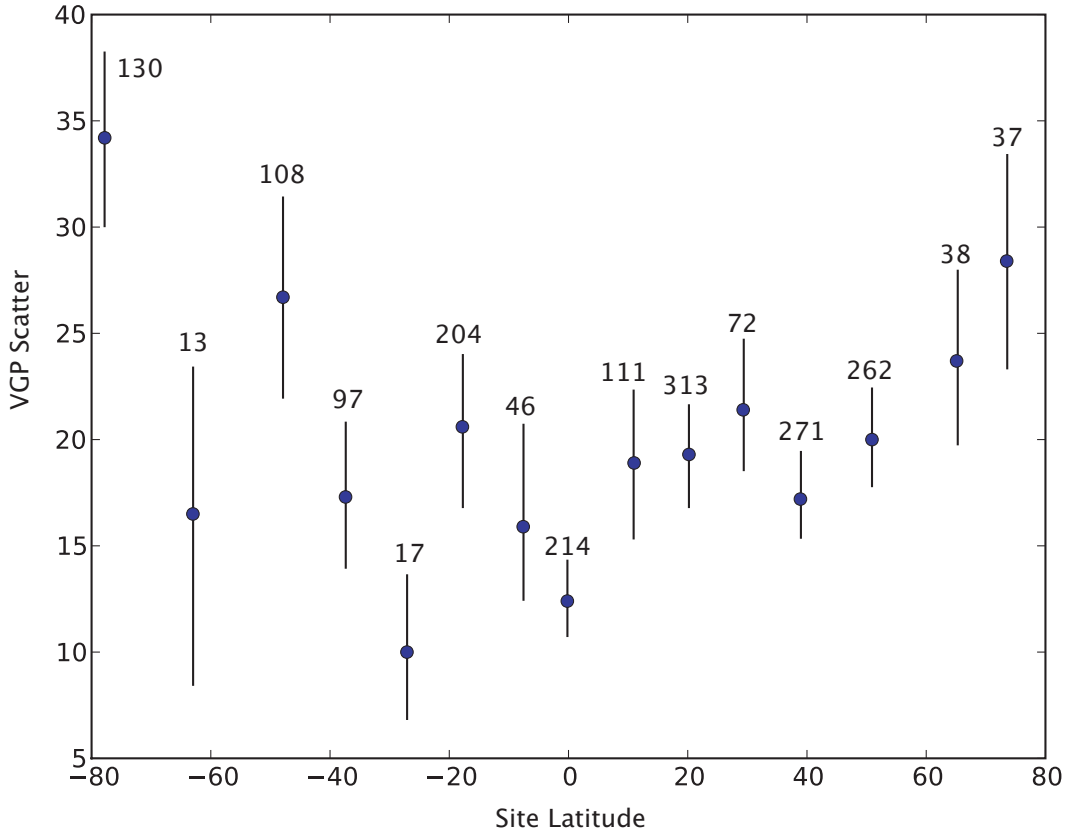

Figure 1.6: Scatter of PSV10 studies, binned in 10° bins, along with the number of studies in each bin.

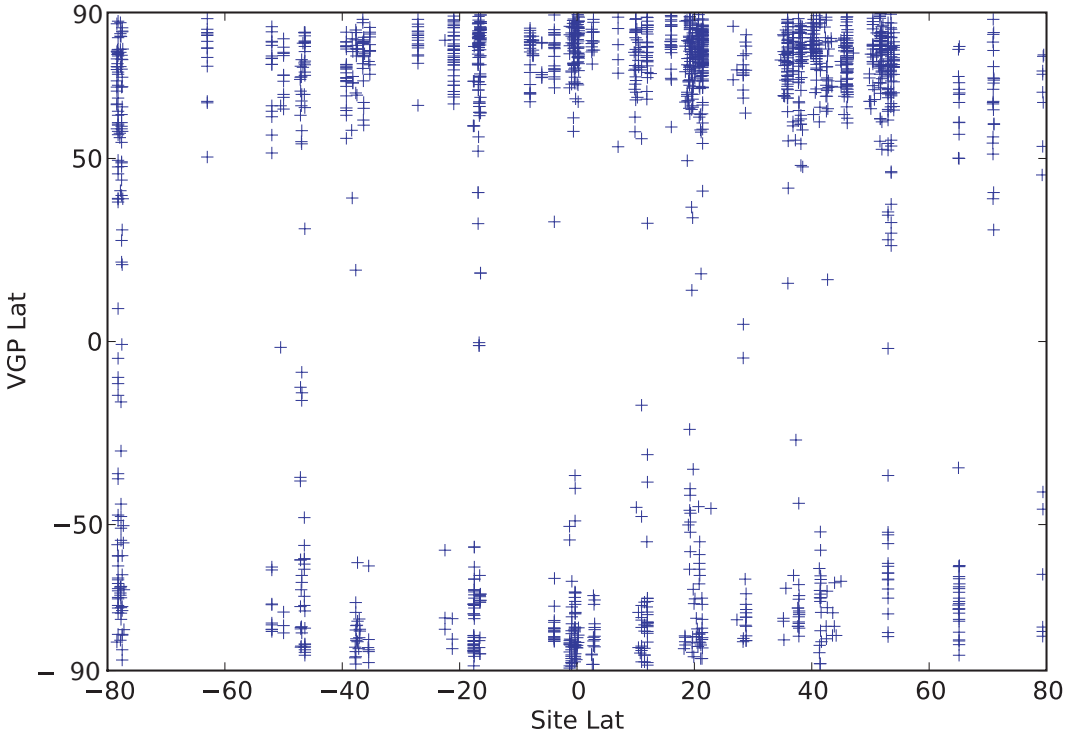

Figure 1.7: VGP latitudes vs. site latitude for individual PSV10 sites.

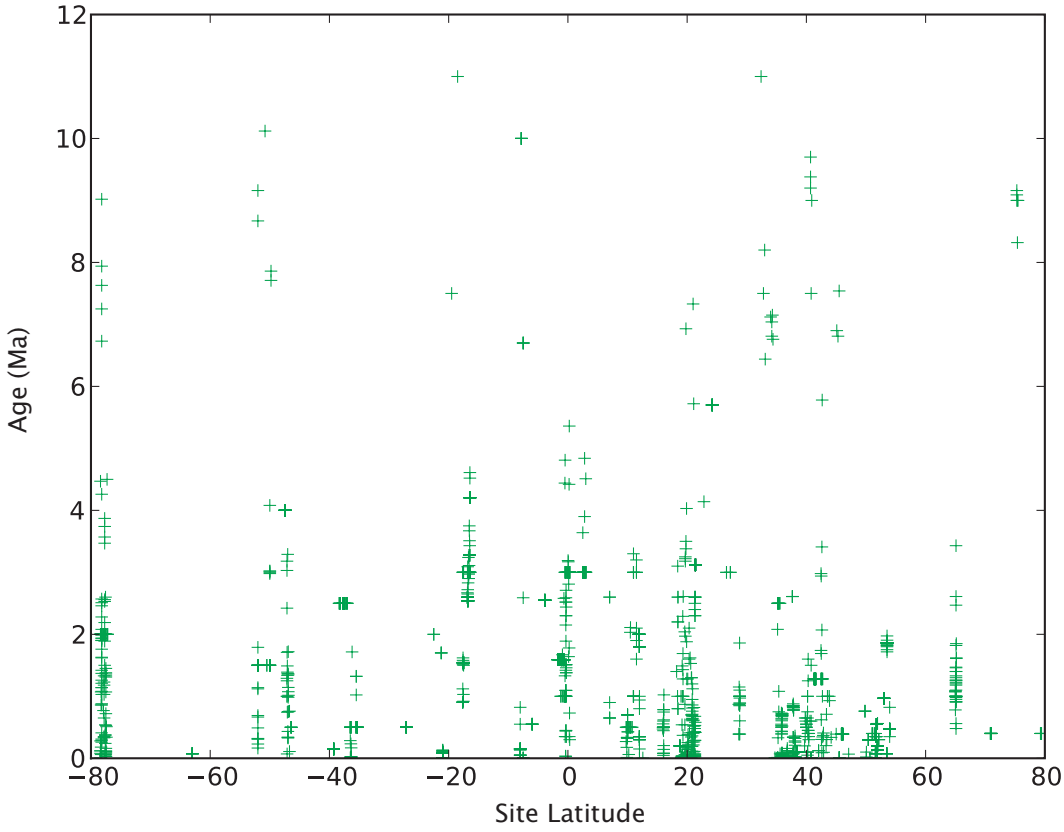

Figure 1.8: Average age of each site plotted vs. site latitude. Age uncertainties are not plotted due to the high volume of data, however all ages are ≤ 10 Ma, within error.

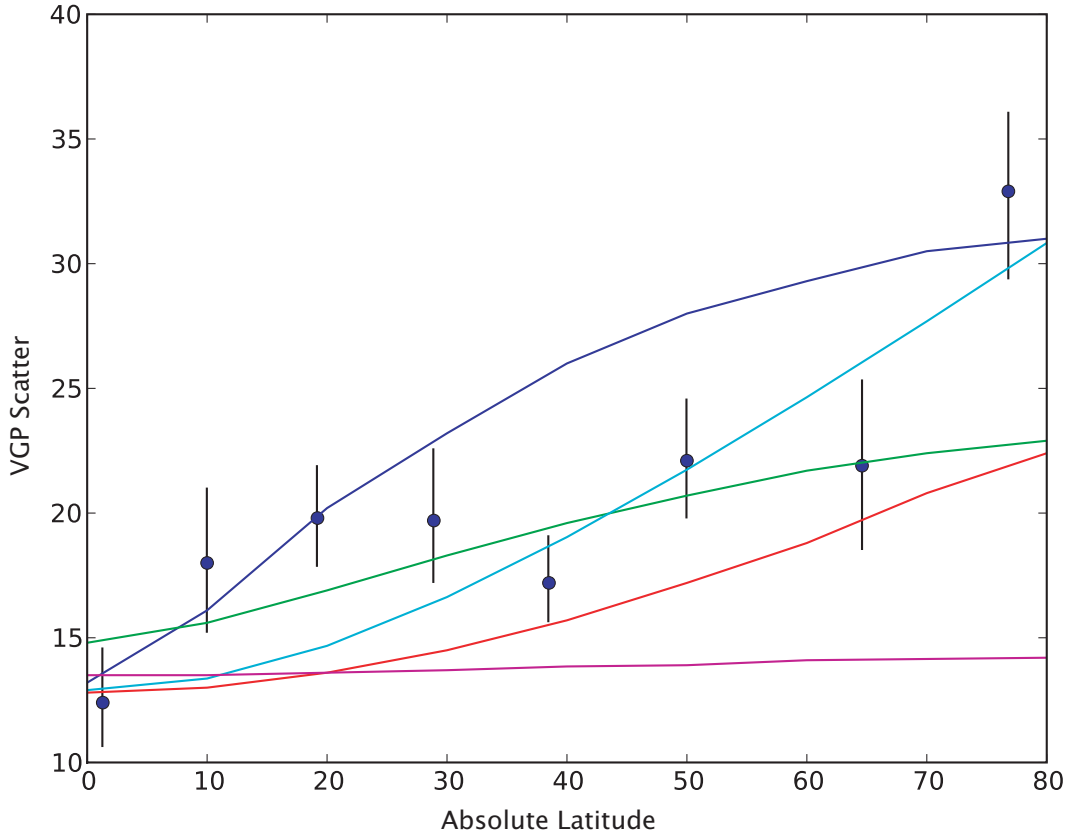

Figure 1.9: Scatter of binned studies (10° bins) vs. absolute site latitude. Models: CP88 (pink), Model G (red), TK03 (green), Model G' (teal), TK03' (blue).

Table 1.3: Spitsbergen site statistics.See Table 1.1 for a description of statistics. Lat*, PLat*, PLon* adjusted for plate motion [Besse and Courtillot, 2002].

Site	Age (ka)	Lat (°N)	Lon (°E)	Dec	Inc	nl/np/N	k	R	$\alpha 95$	VGP Lat	VGP Lon	Lat*	PLat*	PLon*
sp100		79.44	13.33	53.5	82.4	5/2/7	1456.6	6.9966	1.6	77.9	96.1			
sp101		79.44	13.33	85.0	77.8	6/3/9	914.7	8.9929	1.7	65.3	84.6			
sp102		79.39	13.71	212.2	-51.7	3/4/7	373.3	6.9893	3.4	-41.1	337.0			
sp103		79.39	13.70	204.2	-55.7	5/2/7	536.7	6.9907	2.7	-45.8	345.4			
sp104		79.26	13.61	355.5	54.3	5/2/7	1412.6	6.9965	1.7	45.5	198.9			
sp105	8.32±0.17	79.35	14.32	76.8	-88.2	5/3/8	1089.2	7.9950	1.7	-78.0	177.2	75.4	-71.9	191
sp106		79.35	14.32	147.2	-80.7	9/1/10	373.4	9.9772	2.5	-79.2	78.5			
sp107		79.35	14.32	141.7	-82.2	6/3/9	559.9	8.9884	2.2	-80.5	95.5			
sp108		79.35	14.32	338.0	76.6	7/2/9	369.4	8.9810	2.7	73.9	229.9			
sp109	9.16±0.17	79.35	14.32	343.4	72.7	6/3/9	86.9	8.9252	5.7	68.1	218.2	75.3	71.7	223.1
sp110		79.35	14.32	348.9	75.5	5/3/8	385.9	7.9857	2.9	73.0	211.9	75.3	76.8	217.1
sp111	9.09±0.14	79.35	14.32	313.0	64.8	6/3/9	1799.1	8.9964	1.2	53.3	251.4	75.3	55.4	256.2
sp112		79.35	14.32	114.1	-74.5	7/1/8	1625.2	7.9960	1.4	-63.6	100.1	75.4	-63.7	108
sp113		79.52	14.03	331.2	79.8	5/3/8	607.5	7.9909	2.3	78.3	247.5	75.5	80.1	266.5

Table 1.4: Scatter with upper and lower bounds for: No Cutoff, 45°, and Vandamme (cutoff lat).

	No Cutoff	λ_{45}	λ_V
CR	$17.3^{22.0}_{12.6}$	$17.3^{21.9}_{12.9}$	$14.2^{17.0}_{11.1}$ (32.8°)
JM	$29.3^{35.6}_{22.9}$	$23.3^{27.3}_{18.9}$	$27.0^{32.6}_{21.0}$ (53.6°)
SP	$28.1^{35.4}_{20.2}$	$25.7^{32.5}_{17.9}$	$28.1^{35.0}_{20.1}$ (55.6°)

Table 1.5: Summary statistics for all southern hemisphere PSV10 studies. Lat, Lon: average for each study. N is number of sites, S_l^u is calculated scatter for each study, * denotes studies not included in Johnson et al. [2008].

Study	Lat (°N)	Lon (°E)	N Sites	S_l^u	Location	Reference
1	-77.9	165	130	$34.0^{38}_{30.2}$	Antarctica	Lawrence et al., 2009 [55]*
2	-63	299.5	13	$16.5^{23.6}_{9}$	Antarctica	Baraldo et al., 2003 [3]*
3	-51.2	-70.5	40	$23.2^{31.2}_{16.5}$	Patagonia	Mejia et al., 2004 [70]
4	-47.2	51.8	35	$20.2^{25.5}_{14.4}$	Posession Is.	Camps et al., 2001 [8]*
5	-44.3	288.9	33	$36.0^{45.0}_{26.8}$	Argentina	Brown et al., 2004 [6]
6	-39.3	175.5	24	$18.3^{21.3}_{15.2}$	New Zealand	Tanaka et al., 2007 [98]
7	-37.7	144.3	37	$19.9^{27.1}_{12.7}$	Australia	Opdyke and Musgrave, 2004 [80]
8	-36	-69	26	$15.3^{19.1}_{11}$	Argentina	Quidelleur et al., 2009 [83]
9	-35.3	289.5	10	$10.5^{13.1}_{7.9}$	Argentina	Canon-Tapia et al., 1994 [9]*
10	-27.1	250.8	17	$10.0^{13.7}_{6.8}$	Easter Is.	MIki et al., 2008 [72]*
11	-22	208.7	7	$17.2^{25.2}_{9.4}$	Cook-Austral Isds.	Morinaga et al., 1991 [76]
12	-21	55.5	15	$12.3^{14.2}_{10.5}$	Reunion Is.	Rais et al., 1996 [85]
13	-21	55.5	22	$13.8^{16.8}_{10.4}$	Reunion Is.	Chauvin et al., 1991 [12]
14	-16.9	210	44	$24.1^{32.4}_{15.1}$	Society Is.	Yamamoto & Tsunukawa, 2005 [115]*
15	-16.9	210	116	$21.0^{26}_{16.4}$	Society Is.	Yamamoto et al., 2002 [114]
16	-7.5	112.3	34	$13.3^{15.4}_{11.1}$	Java	Elmaleh et al., 2004 [28]*
17	-5.1	327.5	38	$15.4^{20.6}_{11.2}$	Fernando de Noronha Is.	Leonhardt et al., 2003 [56]*
18	-0.9	-90.1	49	$14.0^{17.3}_{10.4}$	Galapagos Is.	Kent et al., in preparation*
19	-0.4	-78.5	48	$17.4^{22.4}_{12.8}$	Ecuador	Opdyket et al., 2006 [78]

Table 1.6: Summary statistics for northern hemisphere PSV10 studies. Lat, Lon: average for each study. N is number of sites, S_l^u is calculated scatter for each study, * denotes studies not included in Johnson et al. [2008]

Study	Avg. Lat.	Avg. Lon.	N Sites	S_l^u	Location	Reference
20	0.7	37	91	$9.6^{10.8}_{8.5}$	Kenya	Opdyke et al., 2010 [79]*
21	7	11	6	$19.4^{29.8}_{8.2}$	Cameroon	Ubangoh et al., 1998 [110]*
22	10.2	-84	27	$17.5^{22}_{12.8}$	Costa Rica	This Study*
23	11.6	41.8	75	$19.4^{24.4}_{13.9}$	Ethiopia	Kidane et al., 2003 [50]*
24	16	298.3	25	$10.9^{14.9}_{7.4}$	French Indies	Carlut et al., 2000 [10]*
25	18.4	265	9	$12.4^{17.2}_{7.4}$	Mexico	Alva-Valdivia et al., 2001 [2]
26	18.8	-110.9	9	$22.8^{29.5}_{15.9}$	Socorro, Mexico	Sbarbori et al., 2009 [88]
27	19.1	260.7	7	$30.1^{48.1}_{10.7}$	Mexico	Morales et al., 2001 [75]
28	19.2	-99.2	10	$2.9^{3.6}_{2.3}$	Mexico	Alva-Valdivia et al., 2005 [1]*
29	19.3	-99.4	10	$31.2^{47.5}_{15.2}$	Mexico	Gonzalez et al., 1997 [35]
30	19.4	204.5	7	$13.0^{15.4}_{10.3}$	Hawaii	Tanaka and Kono, 1991 [101]
31	19.4	-102	22	$20.0^{26.1}_{14.9}$	Mexico	Conte-Fasano et al., 2006 [18]*
32	19.6	204.8	8	$17.4^{21}_{12.6}$	Hawaii	Valet et al., 1998 [112]
33	19.6	260.6	11	$41.4^{46.1}_{35.6}$	Mexico	Mejia et al., 2007 [69]
34	20.1	204.1	10	$13.6^{15.6}_{11.5}$	Hawaii	Brassart et al., 1997 [5]
35	20.2	-97	14	$24.8^{36.2}_{10.8}$	Mexico	Goguitchaichvili et al., 2007 [34]*
36	20.6	203.7	10	$6.5^{8.2}_{4}$	Hawaii	Herrero-Bervera and Valet, 2007 [41]*
37	20.8	203	7	$28.0^{36.9}_{16.2}$	Hawaii	Herrero-Bervera et al., 2000 [38]
38	20.8	-104	15	$19.5^{24.2}_{14.2}$	Mexico	Ceja et al., 2006 [11]*
39	21.1	-104.6	12	$28.4^{42}_{14.4}$	Mexico	Petronille et al., 2005 [82]
40	21.3	202.2	14	$12.2^{16.4}_{8.4}$	Hawaii	Herrero-Bervera and Valet, 2002 [39]
41	21.3	202.1	9	$13.0^{16.5}_{9.4}$	Hawaii	Herrero-Bervera and Valet, 2003 [40]
42	21.4	201.8	82	$14.4^{17.1}_{12}$	Hawaii	Laj and Kissel, 1999 [52]
43	24.2	-16.9	12	$39.4^{59.1}_{15.2}$	Canary Is.	Leonhardt and Soffel, 2006 [57]*
44	26.9	-113	4	$16.2^{20.1}_{9.8}$	Mexico	MOrales et al., 2003 [74]*
45	28.8	342.1	18	$15.7^{18.7}_{12.8}$	Canary Is.	Tauxe et al., 2000 [108]
46	34.1	358.5	11	$35.1^{44.7}_{25.5}$	Spain	Calvo-Rathert et al., 2009 [7]
47	35.3	248.2	14	$16.8^{19.7}_{13.8}$	SW U.S.	Tauxe et al., 2003 [104]
48	35.3	139	3	$10.9^{15.7}_{7.2}$	Japan	Tanaka 1990 [96]
49	35.9	137.5	21	$14.0^{16.3}_{11.5}$	Japan	Tanaka et al., 2007 [97]*
50	35.9	137.5	29	$20.6^{29}_{12.9}$	Japan	Tanaka and Kobayashi, 2003 [99]
51	36.8	12	13	$13.4^{18.4}_{8.8}$	Italy	Zanella 1998 [117]*
52	37.8	334.6	31	$18.2^{22.1}_{14.5}$	Azores	Johnson et al., 1998 [49]
53	38.1	140.5	6	$15.4^{24.3}_{5.8}$	Japan	Otake et al., 1993 [81]
54	38.1	176.5	13	$20.2^{25.8}_{13.8}$	New Zealand	Tanaka et al., 2009 [100]
55	38.4	15.3	14	$10.4^{11.8}_{8.8}$	Italy	Laj et al., 1997 [53]*
56	40.7	4.1	5	$18.5^{24}_{12.9}$	France	Riisager et al., 2000 [86]*
57	45.3	118.7	3	$8.0^{10}_{4.7}$	China	Tanaka et al., 2007 [102]*
58	40.2	44.8	31	$10.4^{13.2}_{7.7}$	Armenia	Solodovnikov, 2000 [92]*
59	40.8	14.4	26	$11.8^{13}_{10.6}$	Italy	Conte-Fasano et al., 2006 [17]*
60	41.6	43.8	37	$19.0^{21.9}_{15.9}$	Georgia	Goguitchaichvili et al., 2000 [33]*
61	43	246.4	23	$22.7^{32}_{14.4}$	NW U.S.	Tauxe et al., 2004 [106]
62	45.5	2.81	7	$16.7^{23.4}_{9}$	France	Salis et al., 1989 [87]*
63	46	121.7	56	$15.3^{17.1}_{13.5}$	NW U.S.	MItchell et al., 1989 [73]
64	50.4	7.3	15	$10.6^{13.2}_{7.9}$	Germany	Schnepp, 1996 [91]*
65	51.1	7.9	3	$12.1^{14.2}_{9.7}$	Germany	Schnepp, 1995 [90]*
66	51.5	-120	50	$17.0^{19.6}_{14.4}$	British Colombia	Mejia et al., 2002 [68]
67	53	-172	55	$27.8^{34.2}_{22.1}$	Alaska	Coe et al., 2000 [15]
68	53.2	190.1	73	$20.6^{25.5}_{15.8}$	Alaska	Stone and Layer, 2006 [94]
69	65.1	-15.5	38	$23.7^{27.7}_{20.2}$	Iceland	Udagawa et al., 1999 [111]*
70	70.9	-8.7	23	$29.3^{36}_{22.1}$	Jan Mayen	This Study*
71	79.4	14	14	$28.5^{35.8}_{19.8}$	Spitsbergen	This Study*

Bibliography

[1] L. Alva-Valdivia. Comprehensive paleomagntic study of a succession of holocene olivine-basalt flow: Xitle volcano (mexico) revisited. *Earth Planets and Space*, 57:839–853, 2005.

[2] L. M. Alva-Valdivia, A. Goguitchaichvili, and J. Urrutia-Fucugauchi. Further constraints for the plio-pleistocene geomagnetic field strength: New results from the los tuxtlas volcanic field. *Earth Planets and Space*, 53:873–881, 2001.

[3] A. Baraldo, A. Rapalini, H. Boehnel, and M. Mena. Paleomagnetic study of deception island, south shetland islands, antarctica. *Geophys. J. Int.*, 153:333–343, 2003.

[4] J. Besse and V. Courtillot. Apparent and true polar wander and the geometry of the geomagnetic field over the last 200 myr. *J. Geophys. Res*, 107:doi:10.1029/2000JB000050, 2002.

[5] J. Brassart, E. Tric, J. P. Valet, and E. Herrero-Bervera. Absolute paleointensity between 60 and 400 ka from the kohula mtn (hawaii). *Earth Planet. Sci. Lett.*, 148:141–156, 1997.

[6] L. Brown, B. Singer, and M. Gorring. Paleomagnetism and ^{40}ar/^{39}ar chronology of lavas from meseta del lago buenos aires, patagonia. *Geochem., Geophys., Geosyst.*, 5:Q01H04, doi:10.1029/2003GC000526, 2004.

[7] M. Calvo-Rathert, A. Goguitchaichvili, and N. Vegas-Tubia. A paleointensity study on middle miocene to pliocene volcanic rocks from south-eastern spain. *Earth Planets and Space*, 61(61-69), 2009.

[8] P. Camps, B. Henry, M. Prevot, and L. Faynot. Geomagnetic paleosecular variation recorded in plio-pleistocene volcanic rocks from possession island (crozet archipelago, southern indian ocean). *Jour. Geophys. Res.*, 106(B2):1961–1971, 2001.

[9] E. Canon-Tapia, E. Herrero-Bervera, and G. P. L. Walker. Flow directions and paleomagnetic study of rocks from the azufre volcano argentina. *J. Geomag. Geoelectr.*, 46:143–159, 1994.

[10] J. Carlut, X. Quidelleur, V. Courtillot, and G. Boudon. Paleomagnetic directions and k/ar dating of 0 to 1 ma lava flows from la guadeloupe island (french west indias): Implications for time-averaged field models. *J. Geophys. Res.*, 105(B1):835–849, 2000.

[11] M. Ceja, A. Goguitchaichvili, M. Calvo-Rathert, J. Morales-Contreras, L. Alva-Valdivia, J. Elguera, J. Urrutia-Fucugauchi, and H. Delgado-Granados. Paleomagnetism of the pleistocene tequila volcanic field (western mexico). *Earth Planets and Space*, 58(1349-1358), 2006.

[12] A. Chauvin, P. Y. Gillot, and N. Bonhommet. Paleointensity of the earths magnetic field recorded by two late quaternary volcanic sequences at the island of la reunion (indian ocean). *Journal of Geophysical Research*, 96(B2):1981–2006, 1991.

[13] B. Clement. Assessing the fidelity of palaeomagnetic records of geomagnetic reversal. *Phil. Trans. R. Soc. Lond.*, 358:1049–1064, 2000.

[14] R. Coe, L. Hongre, and A. Glatizmaier. An examination of simulated geomagnetic reversals from a palaeomagnetic perspective. *Phil. Trans. R. Soc. Lond.*, 358:1141–1170, 2000.

[15] R. Coe, X. Zhao, J. Lyons, C. Pluhar, and E. Mankinen. Revisiting the 1964 collection of nunivak lava flows. *EOS Trans. AGU*, 81(48):Fall Meeting Suppl., Abstract GP62A–06, 2000.

[16] C. Constable and R. L. Parker. Statistics of the geomagnetic secular variation for the past 5 m.y. *J. Geophys. Res.*, 93:11569–11581, 1988.

[17] G. Conte-Fasano, J. Urrutia-Fucugauchi, A. Goguitchaichvili, A. Incoronato, and P. Tiano. Lava identification by paleomagnetism: a case study and some problems surrounding the 1631 eruption of mt. vesuvius, italy. *Earth Planets and Space*, 58:1061–1069, 2006.

[18] G. Conte-Fasano, J. Urrutia-Fucugauchi, A. Goguitchaichvili, and J. Morales-Contreras. Low-latitude paleosecular variation and the time-averaged field during the late pliocene and quaternary- paleomagnetic study of the michoacan-guanajuato volcanic field, central mexico. *Earth Planets and Space*, 58:1359–1371, 2006.

[19] A. Cox. Research note: Confidence limits for the precision parameter, k. *Geophys. J. Roy. Astron. Soc*, 17:545–549, 1969.

[20] A. Cox. Latitude dependence of the angular dispersion of the geomagnetic field. *Geophys. J. Roy. Astron. Soc*, 20:253–269, 1970.

[21] K. Creer. The dispersion of the geomagnetic field due to secular variation and its determination for remote times from paleomagnetic data. *J. Geophys. Res*, 67:3461–3476, 1962.

[22] K. Creer, E. Irving, and A. Nairn. Palaeomagnetism of the great whin sill. *Geophys. J. Int.*, 2:306–323, 1959.

[23] V. Debaille, R. Tronnes, A. Brandon, T. Waight, D. Graham, and C.-T. Lee. Primitive off-rift basalts from iceland and jan mayen: Os-isotope evidence for a mantle source containing enriched subcontinental lithosphere. *Geochimica et Cosmochimica Acta*, 73:3423–3449, 2009.

[24] C. DeMets, R. G. Gordon, D. F. Argus, and S. Stein. Effect of recent revisions to the geomagnetic reversal time scale on estimates of current plate motions. *Geophys. Res. Lett.*, 21:2191–2194, 1994.

[25] J. Dewey and R. Strachan. Changing silurian-devonian relative plate motion in teh caledonides: sinistral transpression to sinistral transtension. *Journal of the Geological Society*, 160:219–229, 2003.

[26] R. Doell and A. Cox. Pacific geomagnetic secular variation. *Science*, 171:248–254, 1971.

[27] M. Drummond, M. Bordelon, J. Debor, M. Defant, H. Bellon, and M. Feigenson. Igneous petrogenesis and tectonic setting of plutonic and volcanic-rocks of the cordillera de talamanca, costa-rica panama, central american arc. *The American Journal of Science*, 295(7):875–919, 1995.

[28] A. Elmaleh, J. P. Valet, X. Quidelleur, A. Solihin, H. Bouquerel, T. Tesson, E. Mulyadi, A. Khokhlov, and A. Wirakusumah. Palaeosecular variation in java and bawean islands (indonesia) during the brunhes chron. *Geophys. J. Int.*, 157:441–454, 2004.

[29] R. A. Fisher. Dispersion on a sphere. *Proc. Roy. Soc. London, Ser. A*, 217:295–305, 1953.

[30] F. Fitch, R. Grasty, and J. Miller. Potassium-argon ages of rocks from jan mayen and an outline of its volcanic history. *Nature*, 207(1349-1351), 1965.

[31] F. Fitch, A. Nairn, and C. Talbot. Palaeomagnetic studies on rocks from north jan mayen. *Norsk Polarinstitutt*, pages 49–60, 1963.

[32] P. B. Gans. Costa rica dates. *Personal Communication*, 2010.

[33] A. Goguitchaichvili, A. Calvob, M. Sologashvilic, D. Alvaa, and J. Urrutia-Fucugauchi. Paleomagnetism of georgian plio-quaternary volcanic provinces (southern caucasus): a pilot study. *Comptes Rendus de l'Academie des Sciences, Seris IIa: Sciences de la Terre et des Planetes*, 331(683-690), 2000.

[34] A. Goguitchaichvili, M. Petronille, B. Henry, L. Alva-Valdivia, J. Morales, and J. Urrutia-Fucugauchi. Paleomagnetisn of the eastern alkaline province (mexico): contribution to the time-averaged field global database and geomagnetic instability time scale. *Earth Planets and Space*, 59:775–783, 2007.

[35] S. Gonzalez, G. Sherwood, H. Bhnel, and E. Schnepp. Palaeosecular variation in central mexico over the last 30,000 years: the record from lava flows. *Geophysical Journal International*, 130:201–219, 1997.

[36] W. Harland. The geology of svalbard. *Geological Society of London Memoir*, 17, 1997.

[37] C. Harrison. Latitudinal signature of earth's magnetic field variation over the last 5 million years. *Geochem. Geophys. Geosyst.*, 10(2), 2009.

[38] E. Herrero-Bervera, J. Margas-Vinuela, and J.-P. Valet. Paleomagnetic study of the ages of lavas on the island of lanai'i, hawai'i. *Journal of Volcanology and Geothermal Research*, 104:21–31, 2000.

[39] E. Herrero-Bervera and J.-P. Valet. Paleomagnetic secular variation of the honolulu volcanic series (33-700 ka), o'hau (hawaii). *Physics of the Earth and Planetary Interiors*, 133:83–97, 2002.

[40] E. Herrero-Bervera and J.-P. Valet. Persistent anomalous inclinations recorded in the koolau volcanic series on the island of oahu (hawaii, usa) between 1.8 and 2.6 ma. *Earth and Planetary Science Letters*, 212:443–456, 2003.

[41] E. Herrero-Bervera and J. P. Valet. Holocene paleosecular variation from dated lava flows on maui (hawaii). *Physics of the Earth and Planetary Interiors*, 61:267–280, 2007.

[42] P. Imsland. The geology of the volcanic island jan mayen arctic ocean. *Nordic Volcanological Institute*, 1978.

[43] P. Imsland. The petrology of the volcanic island jan mayen arctic ocean. *Nordic Volcanological Institute*, 1980.

[44] E. Irving and M. Ward. A statistical model of the geomagnetic field. *Pageoph*, 57:47–52, 1964.

[45] A. Jackson, A. R. T. Jonkers, and M. R. Walker. Four centuries of geomagnetic secular variation from historical records. *Phil Trans Roy Soc London, Series A*, 358(1768):957–990, 2000.

[46] M. Jelenska. Remanent magnetization of permian sediments from central and southern spitsbergen. *Acta Geophysica Polonica*, 35(3):255–276, 1987.

[47] C. L. Johnson and C. G. Constable. The time-averaged geomagnetic field as recorded by lava flows over the last 5 myr. *Geophys. J. Int.*, 122:489–519, 1995.

[48] C. L. Johnson, C. G. Constable, L. Tauxe, R. Barendregt, L. Brown, R. Coe, P. Layer, V. Mejia, N. Opdyke, B. Singer, H. Staudigel, and D. Stone. Recent investigations of the 0-5 ma geomagnetic field recorded in lava flows. *Geochemistry, Geophysics, Geosystems*, 9:Q04032, doi:10.1029/2007GC001696, 2008.

[49] C. L. Johnson, J. R. Wijbrans, C. G. Constable, J. Gee, H. Staudigel, L. Tauxe, V. H. Forjaz, and M. Salgueiro. ^{40}ar/^{39}ar ages and paleomagnetism of sao miguel lavas, azores. *Earth and Planetary Science Letters*, 160(3-4):637–649, 1998.

[50] T. Kidane, V. Courtillot, I. Manighetti, L. Audin, P. Lahitte, X. Quidelleur, P. Y. Gillot, Y. Gallet, J. Carlut, and T. Haile. New paleomagnetic and geochronologic results from ethiopian afar: Block rotations linked to rift overlap and propagation and determination of a similar to 2 ma reference pole for stable africa. *Journal of Geophysical Research-Solid Earth*, 108(B2), 2003.

[51] J. L. Kirschvink. The least-squares line and plane and the analysis of paleomagnetic data. *Geophys. Jour. Roy. Astron. Soc.*, 62:699–718, 1980.

[52] C. Laj and C. Kissel. Geomagnetic field intensity at hawaii for the last 420 kyr from the hawaii scientific drilling project core, big island, hawaii. *Jour. Geophys. Res.*, 104(B7):15317–15338, 1999.

[53] C. Laj, A. Rais, J. Surmont, P. Y. Gillot, H. Guillou, C. Kissel, and E. Zanella. Changes of the geomagnetic field vector obtained from lava sequences on the island of vulcano (aeolian islands, sicily). *Phys. Earth Planet. Inter.*, 99:161–177, 1997.

[54] K. P. Lawrence, C. G. Constable, and C. L. Johnson. Paleosecular variation and the average geomagnetic field at +/- 20 degrees latitude. *Geochemistry Geophysics Geosystems*, 7(Q07007):doi:10.1029/2005GC001181, 2006.

[55] K. P. Lawrence, L. Tauxe, H. Staudigel, C. Constable, A. Koppers, W. C. McIntosh, and C. L. Johnson. Paleomagnetic field properties near the southern hemisphere tangent cylinder. *Geochem. Geophys. Geosyst.*, 10, Q01005:doi:10.1029/2008GC00207, 2009.

[56] R. Leonhardt, J. Matzka, and E. Menor. Absolute paleointensites and paleodirections of miocene and pliocene lavas from fernando de noronha, brazil. *Phys. Earth Planet. Int.*, 139:285–303, 2003.

[57] R. Leonhardt and H. Soffel. The growth, collapse and quiesence of teno volcano, tenerife: new constraints from paleomagnetic data. *Int. J. Earth. Sci.*, 95:1053–1064, 2006.

[58] N. Lyberis and G. Manby. Continental collision and lateral escape deformation in the lower and upper crust: An example from caledonide svalbard. *Tectonics*, 18(1):40–63, 1999.

[59] H. Maher, A. Braathen, S. Bergh, W. Dallman, and W. Harland. Tertiary or cretaceous age for spitsbergen's fold-thrust belt on the barents shelf. *Tectonics*, 14(6):1321–1326, 1995.

[60] A. Maloof, G. Halverson, J. L. Kirschvink, D. Schrag, B. Weiss, and P. Hoffman. Combined paleomagnetic, isotopic, and stratigraphic evidence for true polar wander from the neoprotozoic akademikerbreen group, svalbard, norway. *GSA Bulletin*, 118(9/10):1099–1124, 2006.

[61] M. W. McElhinny and P. L. McFadden. Palaeosecular variation over the past 5 myr based on a new generalized database. *Geophys. J. Int.*, 131:240–252, 1997.

[62] M. W. McElhinny and P. L. McFadden. Paleomagnetism: Continents and oceans. *San Diego: Academic Press*, 2000.

[63] M. W. McElhinny, P. L. McFadden, and R. T. Merrill. The time-averaged paleomagnetic field 0-5 ma. *J. Geophys. Res.*, 101(B11):25007–25027, 1996.

[64] M. W. McElhinny and R. T. Merrill. Geomagnetic secular variation over the past 5 m.y. *Review of Geophysical Space Phys.*, 13:687–708, 1975.

[65] P. McFadden, R. Merrill, M. McElhinny, and S. Lee. Reversals of the earth's magnetic field and temporal variations of the dynamo families. *Jour. Geophys. Res.*, 96:3923–3933, 1991.

[66] P. L. McFadden and M. W. McElhinny. The combined analysis of remagnetization circles and direct observations in paleomagnetism. *Earth Planet. Sci. Lett.*, 87:161–172, 1988.

[67] P. L. McFadden, R. T. Merrill, and M. W. McElhinny. Dipole/quadrupole family modeling of paleosecular variation. *J. Geophys. Res*, 93:11583–11588, 1988.

[68] V. Mejia, R. Barendregt, and N. Opdyke. Paleosecular variation of brunhes age lava flows from british columbia, canada. *Geochem., Geophys., Geosyst.*, 3:DOI number 10.1029/2002GC000353, 2002.

[69] V. Mejia, H. Boehnel, N. Opdyke, M. Otega-Rivera, J. Lee, and J. Arnanda-Gomez. Paleosecular variation and time-averaged field recorded in late piocene-holocene lava flows from mexico. *Geochemistry Geophysics Geosystems*, 6:doi:10.1029/2004GC000871, 2005.

[70] V. Mejia, N. Opdyke, J. Vilas, B. Singer, and J. Stoner. Plio-pleistocene time-averaged field in southern patagonia recorded in lava flows. *Geochem. Geophys. Geosyst.*, 5, 2004.

[71] D. Mertz, W. Sharp, and K. Haase. Volcanism on the eggvin bank (central norwegian-greenland sea, latitude 71°: age, source, and relationship to the iceland and putative jan mayen plumes. *Journal of Geodynamics*, 38:57–83, 2004.

[72] M. Miki, S. Inokuchi, S. Yamaguchi, J. Matsuda, N. Nagao, N. Isezaki, and K. Yaskawa. Geomagnetic paleosecular variation in easter island, the southeast pacific. *Phys. Earth Planet. Int.*, 129:205–243, 1998.

[73] R. Mitchell, D. Jaeger, J. Diehl, and P. Hammond. Paleomagnetic results from theindian heaven volcanic field, south-central washington. *Geophysical Journal*, 97(381-390), 1989.

[74] J. Morales, A. Goguitchaichvili, E. Canon-Tapia, and R. Negrete. Further absolute geomagnetic paleointensities from baja california: evaluation of pliocene and early/middle pleistocene data. *C.R. Geoscience*, 335:995–1004, 2003.

[75] J. Morales, A. Goguitchaichvili, and J. Urrutia-Fucugauchi. A rock-magnetic and paleointensity study of some mexican volcanic lava flows during the latest pleistocene to the holocene. *Earth Planets and Space*, 53(9):893–902, 2001.

[76] H. Morinaga, S. Yamaguchi, M. Hyodo, H. Inokuchi, N. Isezaki, and K. Yaskawa. Paleomagnetism of volcanic rocks from rarotonga and rurutu, the cook-austral island chain. *Journal of Geomagnetism and Geoelectricity*, 43(12):989–1006, 1991.

[77] J. Nawrocki. Paleomagnetism of permian through early triassic sequences in central spitsbergen: Implications for paleogeography. *Earth and Planetary Science Letters*, 169:59–70, 1999.

[78] N. Opdyke, M. Hall, V. Mejia, K. Huang, and D. Foster. The time-averaged field at ecuador: results from the equator. *Geochem. Geophys. Geosyst.*, 7:doi:10.1029/2005GC001221, 2006.

[79] N. Opdyke, D. V. Kent, K. Huang, D. Foster, and J. Patel. Equatorial paleomagnetic time-averaged field results from 0-5 ma lavas from kenya and the latitudinal variation of angular dispersion. *Geochem. Geophys. Geosyst.*, 11, 2010.

[80] N. Opdyke and R. Musgrave. Paleomagnetic results from the newer volcanics of victoria: Contribution to the time averaged field initiative. *Geochem., Geophys., Geosyst.*, 5, Q03H09:doi:10.1029/2003GC000632, 2004.

[81] H. Otake, H. Tanaka, M. Kono, and K. Saito. Paleomagnetic study of pleistocene lavas and dykes of the zao volcano group japan. *J. Geomag. Geoelect.*, 45, 1993.

[82] M. Petronille, A. Goguitchaichvili, B. Henry, L. Alva-Valdivia, J. Rosas-Elguera, J. Urrutia-Fucugauchi, M. Rodriquez Ceja, and M. Calvo-Rathert. Paleomagnetism of ar-ar dated lava flows from the ceboruco-san pedro volcanic field (western mexico): Evidence for the matuyama-brunhes transition precursor and a fully reversed geomagnetic event in the brunhes chron. *Journal of Geophysical Research*, 110(B08101):doi:10.1029/2004JB003321, 2005.

[83] X. Quidelleur, J. Carlut, P. Tchilinguirian, A. Germa, and P. Y. Gillot. Paleomagnetic directions from mid-latitude sites in the southern hemisphere (argentina): Contribution to time averaged field models. *Phys. Earth Planet. Int.*, 172:199–209, 2009.

[84] X. Quidelleur and v. Courtillot. On low-degree spherical harmonic models of paleosecular variation. *Phys. Earth Planet. Int.*, 95:55–77, 1996.

[85] A. Rais, C. Laj, J. Surmont, P. J. Gillot, and H. Guillou. Geomagnetic field intensity between 70 000 and 130 000 years b.p. from a volcanic sequence on la reunion, indian ocean. *Earth Planet.Sci.Letters*, 140:173–189, 1996.

[86] J. Riisager, R. Perrin, P. Riisager, and G. Ruffet. Paleomagnetism, paleointensity and geochronology of miocene basalts and baked sediments from velay oriental, french massif central. *J. Geophys. Res*, 105(B1):883–896, 2000.

[87] J. S. Salis, N. Bonhommet, and S. Levi. Paleointensity of the geomagnetic field from dated lavas of the chaine des puys, france 1.7-12 thousand years before present. *J. Geophys. Res.*, 94:15771–15784, 1989.

[88] E. Sbarbori, L. Tauxe, A. Gogichaishvili, J. Urrutia-Fucugauchi, and W. Bohrson. Paleomagnetic behavior of volcanic rocks from isla socorro, mexico. *Earth Planets and Space*, page in press, 2009.

[89] J.-G. Schilling, R. Kingsley, D. Fontignie, R. Poreda, and S. Xue. Dispersion of the jan mayen and iceland mantle plumes in the arctic: A he-pb-nd-sr isotope tracer study of basalts from the kolbeinsey, mohns, and knipovich ridges. *Jour. Geophys. Res.*, 104(B5):10543–10569, 1999.

[90] E. Schnepp. Paleointensity study of quaternary east eifel phonolitic rocks (germany). *Geophys. J. Int.*, 121:627–633, 1995.

[91] E. Schnepp. Geomagnetic paleointensities derived from volcanic rocks of the quaternary east eifel volcanic field, germany. *Phys. Earth Planet. Inter.*, 94:23–41, 1996.

[92] G. Solodovnikov. Geomagnetic field paleointensity oin the pleistocene determined from extrusive rocks in armenia. *Izvest. Phys. Solid Earth*, 36:468–475, 2000.

[93] A. Stephenson. Three-axis static alternating field demagnetization of rocks and the identification of nrm, gyroremanent magnetization, and anisotropy. *J. geophys. Res*, 98:373–381, 1993.

[94] D. Stone and P. Layer. Paleosecular variation and gad studies of 0-2 ma flow sequences from the aleutian islands, alaska. *Geochem. Geophys. Geosyst.*, 7:doi:10.1029/2005GC001007, 2006.

[95] M. Talwani and O. Eldholm. Evolution of the norwegian-greenland sea. *Geol. Soc. Amer. Bull.*, 88:969–999, 1977.

[96] H. Tanaka. Paleointensity high at 9000 years ago from volcanic rocks in japan. *J. Geophys. Res.*, 95:17517–17531, 1990.

[97] H. Tanaka, R. Kamizaki, and Y. Yamamoto. Palaeomagnetism of the older ontake volcano, japan: contributionsto teh palaeosecular variation for 750-400 ka, the lower half of the brunhes chron. *Geophys. J. Int.*, 169:81–90, 2007.

[98] H. Tanaka, K. Kawamura, K. Nagao, and B. Houghton. K-ar ages and paleosecular variation of direction and intensity from quaternary lava sequences in the ruapehu volcano, new zealand. *Journal of Geomagnetism and Geoelectricity*, 49:587–599, 1997.

[99] H. Tanaka and T. Kobayashi. Paleomagnetism of the late quaternary ontake volcano, japan: directions, intensities, and excursions. *Earth Planets and Space*, 55(4):189–202, 2003.

[100] H. Tanaka, N. Komuro, and G. Turner. Palaeosecular variation for 0.1-21 ka from okataina volcanic centre, new zealand. *Earth Planets and Space*, 61:213–225, 2009.

[101] H. Tanaka and M. Kono. Preliminary results and reliability of palaeointensity studies on historical and c^{14} dated hawaiian lavas. *J. Geomag. Geoelect.*, 43:375–388, 1991.

[102] H. Tanaka, N. Takahashi, and Z. Zheng. Paleointensities from tertiary basalts, inner mongolia and hebei province, northeastern china. *Earth Planets and Space*, 59:747–754, 2007.

[103] L. Tauxe. Essentials of paleomagnetism. *University of California Press*, page 489, 2010.

[104] L. Tauxe, C. Constable, C. Johnson, W. Miller, and H. Staudigel. Paleomagnetism of the southwestern u.s.a. recorded by 0-5 ma igneous rocks. *Geochemistry Geophysics Geosystems*, page doi: 10.1029/2002GC000343, 2003.

[105] L. Tauxe and D. V. Kent. A simplified statistical model for the geomagnetic field and the detection of shallow bias in paleomagnetic inclinations: Was the ancient magnetic field dipolar? In e. a. Channell, J.E.T., editor, *Timescales of the Paleomagnetic Field*, volume 145, pages 101–116. American Geophysical Union, Washington, D.C., 2004.

[106] L. Tauxe, C. Luskin, P. Selkin, P. B. Gans, and A. Calvert. Paleomagnetic results from the snake river plain: Contribution to the global time averaged field database. *Geochem., Geophys., Geosyst.*, Q08H13:doi:10.1029/2003GC000661, 2004.

[107] L. Tauxe and H. Staudigel. Strength of the geomagnetic field in the cretaceous normal superchron: New data from submarine basaltic glass of the troodos ophiolite. *Geochem. Geophys. Geosyst.*, 5(2):Q02H06, doi:10.1029/2003GC000635, 2004.

[108] L. Tauxe, H. Staudigel, and J. Wijbrans. Paleomagnetism and ^{40}ar/^{39}ar ages from la palma in the canary islands. *Geochem. Geophys. Geosyst.*, 1:2000GC000063 [6717 words, 8 figures, 3 tables, 4 appendix tables], 2000.

[109] T. Torsvik, R. Van der Voo, J. Meert, J. Mosar, and H. Walderhaug. Reconstructions of the continents around the north atlantic at about the 60th parallel. *Earth and Planetary Science Letters*, 187:55–69, 2001.

[110] R. Ubangoh, I. Pacca, and J. Nyobe. Paleomagnetism of the continental sector of the cameroon volcanic line, west africa. *Geophys. J. Int.*, 135:362–374, 1998.

[111] S. Udagawa, H. Kitagawa, A. Gudmundsson, O. Hiroi, T. Koyaguchi, H. Tanaka, L. Kristjansson, and M. Kono. Age and magnetism of lavas in jökuldalur area, eastern iceland: Gilsá event revisited. *Phys. Earth Planet. Int.*, 115:147–171, 1999.

[112] J. P. Valet, E. Tric, E. Herrero-Bervera, L. Meynadier, and J. Lockwood. Absolute paleointensity from hawaiian lavas younger then 35 ka. *Earth and Planetary Science Letters*, 161:19–32, 1998.

[113] D. Vandamme. A new method to determine paleosecular variation. *Phys. Earth Planet. Int.*, 85:131–142, 1994.

[114] Y. Yamamoto, K. Shimura, H. Tsunakawa, T. Kogiso, K. Uto, H. Barsczus, H. Oda, T. Yamazaki, and E. Kikawa. Geomagnetic paleosecular variation for the past 5 ma in the society islands, french polynesia. *Earth, Planets and Space*, 54:797–802, 2002.

[115] Y. Yamamoto and H. Tsunakawa. Geomagnetic field intensity during the last 5 myr: Ltd-dht shaw palaeointensities from volcanic rocks of the society islands, french polynesia. *Geophys. J. Int.*, 162(1):79–114, 2005.

[116] Y. Yu, L. Tauxe, and A. Genevey. Toward an optimal geomagnetic field intensity determination technique. *Geochemistry, Geophysics, Geosystems*, 5(2):Q02H07, doi:10.1029/2003GC000630, 2004.

[117] E. Zanella. Paleomagnetism of pleistocene volcanic rocks from pantelleria island (sicily channel), italy. *Physics of the Earth and Planetary Interiors*, 108:291–303, 1998.